



**The development, characterization, and cellular response of  
a novel electroactive nanostructured composite for  
electrical stimulation of neural cells**

Journal:	<i>Biomaterials Science</i>
Manuscript ID:	BM-ART-05-2014-000168.R2
Article Type:	Paper
Date Submitted by the Author:	26-Jun-2014
Complete List of Authors:	Misra, R.D.K.; University of Louisiana, Depan, D.; University of Louisiana at Lafayette, Biomaterials and Biomedical Engineering

**The development, characterization, and cellular response  
of a novel electroactive nanostructured composite  
for electrical stimulation of neural cells**

D. Depan, R.D.K. Misra \*

Biomaterials and Biomedical Engineering Research Laboratory,  
Center for Structural and Functional Materials,  
University of Louisiana at Lafayette, P.O. Box 44130, Lafayette, LA 70504, USA

**Abstract**

Electrical stimulation is a primary method to repair or restore neurological functions. In this regard, we describe the underlying strategy, chemical/structural design, and gifted attributes of a novel nanostructured electroactive composite electrode comprising of organic (highly conducting polymer) – inorganic (carbon nanotubes). The electrode was characterized in terms of electrical properties, structure and neural cell response. First, the electrical probe was robust and characterized by low impedance, high charge injection capacity, and is biocompatible to facilitate cellular interactions. Second, the combination of *in vitro* experiments, fluorescence, and electron microscopy of electrically stimulated cells (NB-39-Nu human neuroblastoma cells) at different applied electric field strength demonstrated that the electrochemically synthesized hybrid nanostructured coating is conducive to neurite growth. Third, the study on the effects of electrical field strength on protein synthesis and mechanism implied cell-to-cell communication based on the change in the regulation of endogenous cytoskeletal proteins, actin, vinculin, and fibronectin involving cell mobility and cell adhesion. The cell-to-cell communication is of significant relevance to functional neuronal circuits in cell translational therapy. Taken together, the results also point to the potential of nanostructured composite for use as substrates to modulate cellular activity via electrical stimulation.

---

\*Corresponding author: R.D.K. Misra, Email: [dmisra@louisiana.edu](mailto:dmisra@louisiana.edu)  
Tel: 001-337-482-6430, Fax 001-337-482-1220

## 1. Introduction and Design Considerations in the Synthesis of an Electroactive Neural Electrode

**1.1 Introduction:** Electrical stimulation of nerve cells is widely employed in neural prostheses (for hearing, vision, and limb movement restoration) [1-4], and in clinical therapy to cure Parkinson's disease [5]. However, functional stimulation especially in the central nervous system requires the use of small electrodes with high current density, which conflicts with the electrochemical safety requirements. Undesirable electrochemical change damages the electrode and may cause abnormalities in neural functions and cell structure [6], primarily because of the contact problems at the electrode/tissue interface.

Neural devices used to repair or restore damaged neurological functions by electrical stimulation or record neural activity from the peripheral or central nervous system (CNS) involves the use of microelectrodes, referred as neural electrodes [7]. The neural interface facilitates smooth exchange of information between the central nervous system and device. These two tasks require transduction of electrical charge via an electrode-electrolyte interface, where the interface is characterized by electrical impedance and the charge injection limit of the interfacial double-layer capacitance [8]. Capacitive charge injection is an ideal mechanism for neural stimulation because no chemical change is induced to either the electrode or the tissue.

In the nervous system, there are neurons and non-neuronal cells, referred as glial cells. A neuron communicates with other neurons by carrying signals over its axon, a projection that is several orders of magnitude longer than the neuron diameter, and transmits the signal to the target neuron using transmitting synapses. Glial cells support neurons with nutrients, protection, neurotransmission, and maintenance of their environment [9].

The neural device consists of a number of microelectrodes arrayed on a substrate with small geometrical size to facilitate excitation of a group of neurons. This aspect is a challenge because microelectrodes have to sustain high current density pulses through the electrode-tissue interface without causing irreversible Faradaic reactions and tissue damage [10]. A viable approach to improve the electrochemical characteristics of microelectrode is to employ a reversible charge injection process either via a double layer capacitive mechanism or through a reversible Faradaic mechanism [7]. However, the functioning of neural microelectrodes is associated with inconsistent performance caused by tissue response [11]. It has been previously noted that the electrodes implanted in the central nervous system get covered with a highly resistive astroglial encapsulation because of inflammatory response, leading to the electrical isolation of the electrodes from the target neurons [12]. This astroglial encapsulation results in the loss of neurons near the electrodes and elevates the electrode impedance and power consumption of the implantable device [13,14]. Thus, current efforts are devoted to the synthesis of superior electrochemical performance and biocompatibility. For electrical stimulation, majority of the neural electrodes are made from stable and corrosion resistant metals, such as platinum, iridium, gold, platinum-iridium alloy, titanium, and stainless steel.

The charge injection capacity (CIC) of an electrode is important in the selection of an electrode material. It is defined as the amount of charge that can be transferred through a specific area ( $C/cm^2$ ) before irreversible corrosion mechanism (electrode dissolution) is initiated [15].

The most widely used electrode is Pt, for instance, in cochlear implant electrodes, because of excellent biostability and corrosion resistance [16]. But, an inherent drawback of Pt is the maximum safe charge injection ( $Q_{inj}$ ) limit of only  $\sim 0.15$   $mC/cm^2$  [17], which limits its application in neural microelectrodes. The bare electrodes are also known to exhibit poor

performance during long-term stimulation and recording because of poor contact with the tissue or due to scar formation. Thus, they are surface modified to improve the electrode functionality. A thin layer of rough and porous coating of conducting material (e.g. carbon) on the surface of neural electrodes increases the effective surface area, improves the efficiency of charge transfer, and favorably modulates the electrode biocompatibility [18].

Neural electrodes are coated with iridium oxide ( $\text{IrO}_2$ ) because of unique properties that favor neural stimulation.  $\text{IrO}_2$ -coated electrodes are non-cytotoxic [19] and have very low impedance and a high charge injection limit. These characteristics enable high levels of charge injection capacity without electrode dissolution or water electrolysis [20]. However,  $\text{IrO}_2$  has poor adhesion to the underlying substrate and may degrade under chronic aggressive stimulation because of inferior structural and chemical stability. Iridium oxide ( $\text{IrO}_2$ ) by itself, is widely acceptable for microelectrodes, because of superior characteristics including good biostability, low impedance at 1 kHz, and high  $Q_{inj}$  limit of  $\sim 4.0 \text{ mC/cm}^2$ . While  $\text{IrO}_2$  electrodes are acceptable, they are generally used as recording electrodes because when used as stimulating electrode, delamination of  $\text{IrO}_2$  film takes place at high stimulation densities, leading to tissue damage and inflammatory response [21,22].

Based on the above discussion, it is expected that the neural electrodes exhibit are characterized by following desired attributes, notably, physical or structural biocompatibility, chemical and biological inertness, electrochemical stability, and high charge injection limit.

In recent years, the general assumption has been that the cell body (soma) of a neuron, which contains the nucleus, is primarily responsible for the synthesis of macromolecules and has limited role in cell-to-cell communication [23]. It is reported that depolarization in neurons could trigger capacitance increase, indicating somatic exocytosis [24]. A group of researchers [25,26]

noted release of pre-loaded transmitters or dyes and pain-related peptides including calcitonin-gene related peptide (CGRP) from the neuron somata in response to the action potential. The somatic secretion provided a method to excite neuron in an autocrine or paracrine fashion via extrasynaptic mechanisms for modulating the activity of neurons and thereby influence the transmission of sensing input to the central nervous system (CNS) and spinal cord [25,26].

**1.2 Design of novel electroactive electrode:** In the attempt to design a chemically and structurally stable and robust electrode for chronic neural stimulation, we have considered Langer's pioneering studies on rat nerve proliferation on polymer polypyrrole substrates [27]. Conducting polymers have been used as components for *in vivo* nerve guides and as coatings to lower the impedance of neural electrodes. The considerations of organic electronic materials are limited to simple polypyrroles and polythiophenes, and furthermore, their covalent modification to enhance biofunction continues to be a challenging task [27].

Hybrids of conducting polymers and hydrogels have recently been explored as soft electroactive coatings for improving the mechanical and electrical performance of metallic implant electrodes. Since, hydrogel fabrication methods generally tend to produce bulky implants, which displace a large volume of tissue, the fabrication of a thin film is a challenging task. To alleviate this aspect, poly (2-hydroethyl methacrylate) (p-HEMA) polymer brushes were grafted to gold electrode followed by poly (3,4-ethylenedioxythiophene) (PEDOT) coating on brushes [28].

There are also reports on organic transistor for stimulation and recording of primary neurons [29]. These organic ultra-thin film transistors were observed to be suitable for good cellular adhesion and efficient coupling of the ionic currents at neural interface [30]. The studies also indicated that astroglial cells play an active role in information processing than previously

anticipated. Elucidating the role of glial cell is expected to identify new targets, thereby enabling the development of effective therapy [31,32]. Organic semiconducting thin films also allowed interaction between astrocytes and biomaterials to be studied from the view point of control and minimization of reactive astrogliosis. Thus, organic transistors provide a new perspective for selective manipulation of astrocyte bioelectrical activity by non-invasive, label-free organic-based, photostimulation approach [33].

In regard to short term effects of electrode insertion on surrounding tissue, Polikov and Bellamkonda [13] studied the effects in terms of cell death (both neuronal and glial), severed neuronal processes and blood vessels, mechanical tissue compression, and collection of debris resulting from cell death. Current theories suggest that glial encapsulation, i.e. gliosis, insulate the electrode from nearby neurons, hinder diffusion, increasing impedance, and extend the distance between the electrode and its nearest target neuron [14].

Based on the above discussion, the design of robust bioelectronic materials that integrate cell adhesive cues and favorable electrical transport incorporating nanostructures (e.g. CNTs, carbon nanohorns, graphene) are envisaged to take the next step toward binding biotic-abiotic interface. This will eliminate the need to modify conductive polymer assemblies with interactive biological functionalities. Given the practical importance of fabricating an ideal electrode that reliably performs for a long period and the need for the electrodes to sense signals emanating from individual neurons, our first focus was to design/fabricate robust electrical probes with the desired attributes outlined above that can be reliably used to stimulate neurons.

In this study, we exploited the attributes of conducting polymer, (poly(3,4-ethylenedioxythiophene): PEDOT) and carbon nanotubes (CNTs) for neural interfacing. PEDOT is a promising conducting polymer because it is characterized by ordered and well-defined

chemical structure [34]. On the other hand, purified CNTs have extraordinary electrical and mechanical strength and are biocompatible. Thus, by incorporating CNTs at small concentrations (0.1 wt.%) in PEDOT, we can accomplish the task of fulfilling biocompatibility and stability requirements of PEDOT as a coating material. This is important because PEDOT coatings delaminate during electrical stimulation. CNTs provide mechanical stability to the electrode during electrical stimulation. Furthermore, CNTs appear to promote neuron differentiation [35,36], stimulate neurite growth [37], enhance neuronal performance and recording [38], and promote neuronal electrical signaling [37]. Thus, they can be advantageously incorporated in conducting polymers [39]. But bare CNT electrodes are not promising because of relatively low charge injection ( $Q_{inj}$ ) limit of 1-1.6 mC/cm<sup>2</sup> [40], when neurons are excited with a capacitive charge-injection mechanism. Thus, it was important for us to synergistically utilize the benefits of both PEDOT and CNTs via co-electrodeposition of CNT-PEDOT on stainless steel electrodes. The synthesis of PEDOT-CNT hybrid nanostructured composite coating on stainless steel electrode culminated in interfacial adhesion, coming from electrostatic and van der Waals interaction in the hybrid polymer-CNT nanostructure (please see section 2).

CNT-PEDOT combination provides electronic cues to influence cell growth and guide repair following severe damage to the central nervous system, which offers innovative therapeutic interventions. The design of the electrode material studied here provides an innovative platform technology with several distinct advantages over other existing electroactive materials. Electrically conductive polymers when doped (in our case CNTs) draw analogies to the neural and cardiac biosystem that rely on electrical conduction.

The objective of the study is to first demonstrate the potential of the proposed design of a robust neural probe based on the required attributes of the electrode, study its characteristics, and

prove its efficacy for electrical stimulation. This was accomplished through combination of conducting polymer and CNTs. Given that the mechanical stability of neural electrode is of prime concern in neural tissue engineering, CNT-PEDOT combination provides the following advantages over other conventional neural probes: (a) chemical and mechanical stability, (b) biocompatibility, (c) promotion of neuronal adhesion and neuronal outgrowth by positively charged polymer, and (d) high charge injection capacity. Furthermore, to understand the cell-to-cell interaction under weak electric field stimulation and regulation of the cytoskeletal proteins is another aspect, which is not well understood and is part of our objective.

## **2. Materials and Experimental Methods**

### **2.1. Materials**

Single-walled carbon nanotubes (CNTs) of length  $\sim 30 \mu\text{m}$  and diameter  $\sim 2 \text{ nm}$  were obtained from Global Nanotech, Mumbai. The monomer, 3,4-ethylenedioxythiophene (EDOT), and phosphate buffered saline (PBS, pH 7.4, 10 mM sodium phosphate and 0.9% NaCl) was purchased from Sigma-Aldrich, USA. All chemicals used were of analytical grade. Sulphuric acid, nitric acid, 1-ethyl-3-(3-dimethyl aminopropyl) carbodiimide (EDC), N-hydroxy succinimide (NHS), and ethanol were obtained from Sigma-Aldrich, USA.

### **2.2. Fabrication of poly(3,4 ethylenedioxythiophene) (PEDOT) CNT-PEDOT-coated electrodes**

Based on the discussion in section 1, CNT-coated austenitic stainless steel electrodes were synthesized using the followed steps: The first step involved functionalization of CNTs. 20 mg of CNTs were dispersed and treated with 50 mL of 1:3 concentrated  $\text{HNO}_3$  and  $\text{H}_2\text{SO}_4$  solution for 3 h while sonicating in an ice bath, to functionalize CNTs through the attachment of  $-\text{COOH}$  groups on the surface of CNTs. The dispersed suspension was kept at  $20^\circ\text{C}$  for  $\sim 12 \text{ h}$ .

After treatment with acid (i.e. functionalization), the CNTs were washed with water and separated by ultracentrifugation (@15000 rpm for five times), until the pH of the solution was neutral. The functionalized CNTs were dried at 60°C.

In the second step, functionalized CNTs were immersed in a mixture consisting of 5 mg/mL of 1-ethyl-3-(3-dimethylaminopropyl) carbodiimide hydrochloride (EDC) and 5 mg/mL of N-hydroxysuccinimide (NHS) for 1 h at room temperature to activate the carboxylic groups. Subsequently, the CNTs were washed with phosphate buffer saline (PBS) and dried at room temperature.

Next, the hybrid CNT-PEDOT nanostructured film was electrodeposited onto austenitic stainless steel electrodes through electropolymerization process using an aqueous solution comprising of 2 mg/mL CNTs and 0.01 mol/L ethylenedioxythiophene (EDOT) monomer. The electrochemical set-up for electropolymerization consisted of a three-electrode system (stainless steel working electrode, platinum counter electrode, and a Ag/AgCl reference electrode) coupled to a potentiostat. The optimized electrochemical parameters to obtain a uniform (CNT-PEDOT) film on stainless electrode were current density of 1 mA/cm<sup>2</sup> for 5 minutes.

To elucidate the effect of CNT, bare CNTs were deposited onto stainless steel electrode without PEDOT. The procedure involved the following: A CNT dispersion (0.2 mg/ml) was made in distilled water by sonicating for 3 h. Identical amount of pyrocatechol violet was added in this dispersion, followed by 1 h stirring at room temperature. This dispersion was used to coat a uniform layer of CNTs onto stainless steel using a potentiostat, as described above in section 2.2.

Considering that CNTs acts as a charge carrier in the electrochemical deposition or electro-polymerization of PEDOT onto stainless steel, bare PEDOT coating on stainless steel

electrode was not possible to fabricate. However, bare stainless steel electrode and CNT-coated stainless steel electrodes were used as controls in the determination of impedance, which is an important aspect in the design of the electroactive electrode.

The nanoscale surface morphology and roughness of bare stainless steel was studied using atomic force microscope (AFM) (Nanoscope TM ® IIIa, Digital Instruments, Santa Barbara, CA.). Atomic force microscopy was carried out using tapping mode to prevent possible damage due to continuous contact. All the scans were made in air and the tip used to study the sample was 'tapping mode etched silicon probe' (TESM). The number of scan lines for an individual image was 512 with 512 points per line. Five images were taken at a number of locations on the sample to ensure that the presented image was a true representative of the topography of the surface.

### **2.3 Study of electrochemical properties of neural electrode**

Cyclic voltammetry and electrochemical impedance spectroscopy (EIS) measurements were carried out using a potentiostat (Princeton Applied Research, USA). In brief, cyclic voltammetry was performed in the potential range of -0.6 and 0.7 V at a scan rate of 100 mV/s in PBS (pH=7.3). The area of the current-voltage plot obtained from the time integral of the current in one cycle of the current-voltage was a measure of the charge storage capacity.

The electrochemical impedance [39-41] was measured in the frequency range of 1-100 kHz using an alternating current sinusoid of 5 mV in amplitude with the direct current potential set at 0 V using a Gamry potentiostat.

The stability of the hybrid CNT-PEDOT nanostructured film on 316 LN stainless steel electrode was studied by two different methods. The first approach involved cyclic voltammetric stimulation with a potentiostat, using a voltage scan from -0.9 to 0.5 V, at a scan rate of 100

mV/s for 3000 cycles [39]. The stimulation was conducted using a programmable multichannel stimulator (Multichannel Systems STG2002). An oscilloscope and the WaveStar program measured and recorded the voltage excursion. In the second approach, the CNT-PEDOT coated stainless steel microelectrode was soaked in PBS for ~14 days, followed by stimulation under a charge balanced, cathodic first, biphasic pulse current at  $0.30 \text{ mC/cm}^2$  at 50 Hz. The impedance at 1000 Hz and cyclic voltametry measurements were periodically monitored for change in the impedance and electrochemical behavior with time.

#### 2.4 Structural morphology of CNT-PEDOT electrode

The microstructure of the CNT-PEDOT film was examined using scanning electron microscope with a Hitachi S-3000 operated at 15 kV. The CNT-PEDOT coated stainless steel probe was dried in an oven at  $80^\circ\text{C}$  for 1 h, followed by sputter coating with gold of ~0.8. nm before characterizing the structure via SEM.

#### 2.5 Cell culture

NB-39-Nu human neuroblastoma cells (neural cell line: ATCC, Manassas VA, USA) were cultured in Dulbecco's modified eagle medium (DMEM) (Gibco BRL, NY, USA) with 10% heat-inactivated fetal bovine serum (FBS; Sigma-Aldrich, St. Louis MO, USA). NB-39-Nu is a human primary neuroblastoma (NB) cell line. They are transformed, neural crest derived cells, capable of unlimited proliferation and differentiation, *in vitro*. The cells retain the ability differentiate into neuronal cell types. This ability of NB cells to proliferate and differentiate makes them an excellent cell line for *in vitro* studies. **Next, neural cells at a density of  $2 \times 10^5$  cells/cm<sup>2</sup>** were plated onto the CNT-PEDOT coated stainless steel microelectrode in a 30 mm culture dish and placed in a 5% CO<sub>2</sub> incubator.

To examine the neurite outgrowth and attachment of cells by scanning electron microscopy, CNT-PEDOT coated stainless steel electrodes were first rinsed with PBS to remove the culture medium and non-adherent cells. Next, they were treated with 2.5% glutaraldehyde for 1 h, followed by the dehydration process. The dehydration process involved soaking of electrodes for 15 minutes in each of the following solutions in the sequence: 30% and 50% ethanol in PBS, 70% and 90% ethanol in water, and 100% ethanol.

The neural cells cultured on PEDOT-CNT-coated stainless steel electrode were electrically stimulated using a function generator for pulse generation which consist of a switching circuit and variable power supply. This in-house set-up can be used to apply variable voltage with a frequency range of 0.3 Hz-1.0 MHz. Prior to electrical stimulation, the neural electrodes were ultrasonically cleaned and autoclaved. Cultured neural cells on electrodes were stimulated for 5-50 mV/mm at a frequency of 100 Hz with a duty cycle of 4%, while keeping the electrodes at least 3 cm apart and keeping the electric field parallel to the cultured cells. The cells were stimulated for 5 min, followed by incubation for 6 h in a humidified CO<sub>2</sub> chamber maintained at 37°C.

## **2.6 Cell viability**

Cell viability of the electrically stimulated cell samples (10 mV/mm) was determined using MTT (3-(4,5-dimethylthiazol-2-yl)-2,5- diphenyltetrazolium bromide) assay (Sigma, St. Louis, USA). The samples were washed with PBS, followed by incubation with fresh culture medium containing MTT (0.5 mg ml<sup>-1</sup> medium) at 37 °C for 4 h in darkness. The unreacted dye was removed and DMSO was added to dissolve the intracellular insoluble purple formazan product into a colored solution. The optical density (OD) of the formazan solution was read

using spectro-photometric plate reader (Bio TEK Instrument, EL-307C) at a wavelength of 570 nm, and the results obtained were expressed as OD after subtraction of the blank.

## **2.7 Cell morphology and cell density analysis**

The neural cell-CNT/PEDOT electrode constructs were washed twice with PBS, followed by fixation with 2% v/v glutaraldehyde in cacodylate buffer (pH 7.4) for 30 min and then washed with PBS. After washing the fixatives, the samples were dried with a graded ethanol series, and then sputter coated with gold prior to the study of morphology by SEM.

The quantification of cell proliferation was done by determining the cell density using the fluorescence micrographs presented in Figure 4. At least five non-overlapping locations on each sample were selected to calculate the average cell density. At least 20 micrographs for each experiment were selected for cell density measurement, using Image J Pro software.

## **2.8 Effect of electrical field on cytoskeletal proteins: Immunocytochemistry and fluorescence microscopy**

After electric field stimulation, the neural cells in the culture dish were fixed for 20 min with 4% paraformaldehyde in PBS (pH 7.4) and rinsed with PBS at least three times using the following protocol [42]. Next, the cells were incubated in PBS solution comprising of 4% normal goat serum (NGS; Vector laboratories, CA, USA), 0.2% Triton X-100, 2% bovine serum albumin (BSA; Sigma- Aldrich, St. Louis MO, USA), 2% FBS (Sigma-Aldrich, St. Louis MO, USA) and primary antibodies for 60 min at room temperature. After washing with PBS, secondary Alexa fluor 568 goat anti-mouse IgG (H + L) and Alexa fluor 488 goat anti-rabbit IgG (H + L) (1:1000, Molecular Probes, OR) were applied to the cells for 60 min at room temperature in the dark followed by rinsing of cells with PBS. To stain the nucleus, DAPI (1:100 dilution) was added to the last PBS buffer wash and cells incubated for 20 min at 20°C and

washed again prior to mounting. Cells were incubated in CO<sub>2</sub> incubator at 37°C for 40 min. After final washing with PBS, cells were mounted with fluorescent mounting medium (DakoCytomation, CA, USA) and covered with glass cover slip. The primary antibodies used and their dilution was as follows: rabbit anti-fibronectin (1:500, Millipore, USA); mouse monoclonal anti-F-actin (1:1000, Millipore, USA); rabbit anti-vinculin (1:500, Millipore, USA). After immunostaining, cells were examined with fluorescence microscope (DMI6000B, Leica, Germany).

Fluorescence micrographs of at least 25 non-overlapping individual regions on each sample were randomly chosen to calculate the fluorescence intensity using Image J software. The neurite outgrowth was quantified by counting the number of neuroblastoma cells bearing neurites and measuring the neurite length in randomly selected SEM micrographs. A total of 10 micrographs were used to quantify neurite outgrowth using Image analysis software (Image J; NIH, Bethesda, MD).

## **2.9 Statistical Analysis**

All the experiments involved a minimum of five samples and five tests were carried out for the cell culture studies. The obtained values in each experiment were normalized with respect to the control samples. Results are expressed as the mean value of at least five replicates  $\pm$  SD (standard deviation). Statistical analysis was carried out using the one-way analysis of variance (ANOVA) with 95% confidence interval. The error bars denote  $\pm$ SD ( $n \geq 5$ ).

## **3. Results and discussion**

It is important to first describe the characteristics of the CNT-polymer electrode used for stimulation prior to discussing cell-to-cell communication and cellular activity.

### 3.1 Structural and electrochemical characteristics

High magnification atomic force micrograph of bare stainless steel and scanning electron micrograph of CNT-PEDOT-coated stainless steel electrode is presented in Figure 1a and b, respectively. Metallographically polished mirror surface of bare stainless steel had atomic scale roughness of  $1.45 \pm 0.21$  nm. The figure shows that CNTs are uniformly dispersed in the PEDOT matrix and are characterized by a network-like structure. This desired structural morphology is attributed to the methodology adopted to fabricate the CNT-PEDOT coated stainless steel electrode. The functionalized CNTs with carboxyl groups were individually dispersed in the aqueous solution. During the electropolymerization of PEDOT in aqueous solution comprising of monomer EDOT and CNTs, the functionalized and negatively charged CNTs with carboxyl groups acted as dopants to neutralize the positive charge present in the backbone of the PEDOT. This facilitates their incorporation in the PEDOT polymer matrix. The combination of highly conducting CNTs with large surface area ( $\sim 1000$  m<sup>2</sup>/g by BET analysis) and conducting PEDOT polymer renders the microelectrode suitable for neural stimulation and in restoring lost or impaired neurological functions.

Furthermore, there was no visible indication of the CNT-PEDOT electrodeposited film experiencing delamination or cracking during neural stimulation at different voltage, and the structural characteristics continued to be similar to the as-synthesized electrode. This behavior is in contrast to PEDOT-PSS coating that experienced delamination during chronic stimulation [43].

The charge storage capacity of CNT-PEDOT coated stainless steel electrode as determined by cyclic voltammetry is presented in Figure 2. A high charge of  $\sim 70$  mC/cm<sup>2</sup> was

obtained at electrodeposition charge of  $\sim 70 \mu\text{C}$  and is preferred for neural stimulation. The underlying reason for high charge storage capacity is CNTs. The CNTs are highly conducting with large surface area such that the network-like distribution of PEDOT-coated CNTs in the PEDOT matrix effectively increases the electrode/electrolyte interface area and increases the conductivity of the film. This renders the deposited polymer highly conducting for subsequent electrodeposition. Another aspect to be noted from Figure 2 is that the charge storage capacity of CNT-PEDOT-coated electrode increases with the electrodeposition charge. This behavior is anticipated because higher electrodeposition charge results in thick and rough film with greater density of electroactive species. Furthermore, the charge capacity increases linearly with electrodeposition charge. This is in contrast to pure PEDOT film, which indicated linear relationship at low electrodeposition charge (thin film) and non-linear at high electrodeposition charge (thick film), when the film becomes dense and contains high density of defects in the lattice [44].

The voltage response of an electrode upon current stimulation is a direct indicator of its charge injection capability. An appropriate or desired neural electrode is characterized by high charge injection capability. The underlying reason being that at a given pulse current it will generate lower electrode voltage and is safe for neural stimulation. The CNT-PEDOT-coated electrodes were examined under pulse stimulation current to evaluate their charge injection capacity. The charge injection limit is defined as the maximum cathodic charge that resulted in cathodic or anodic electrode voltage exceeding 0.6 V versus the Ag/AgCl reference electrode. The average charge injection limit of CNT-PEDOT electrode was  $\sim 2.3 \pm 0.2 \text{ mC/cm}^2$  and is comparable to  $\text{IrO}_2$  electrode. The results indicate that CNT-PEDOT-coated electrodes can

deliver higher charge density without generating high voltage, which is beneficial in preventing detrimental effect on the surrounding tissues.

The impedance of the CNT-PEDOT-coated electrode and the bare stainless steel electrode in the frequency range of 1 and  $10^3$  Hz is presented in Figure 3. In this frequency range, the impedance of the CNT-PEDOT-coated stainless steel electrode was observed to decrease by ~70% from ~30,000 ohm to ~200 ohm. The significant drop is in contrast to the bare stainless steel electrode and is a consequence of CNT-PEDOT-coating on stainless steel. The decrease in impedance can be discussed in terms of a circuit model comprising of a solution resistance ( $S_R$ ) in series with a finite-length warburgh diffusion impedance component of bulk film ( $D_F$ ) and bulk (electronic) capacitance ( $E_C$ ) [45,46]. In this model,  $S_R$  is constant because solution does not change,  $E_C$  depends on the electroactive surface area, and in the high frequency region, the impedance due to  $E_C$  is small, and the impedance is influenced by  $D_F$ . Based on Figure 3, there is insignificant change in impedance in the high frequency range, which is  $D_F$ , implying high conductivity of the CNT-PEDOT electrode material. On the other hand, in the low frequency region,  $E_C$  contributes to impedance.

### **3.2 Cell viability, proliferation and morphological changes in relation to electrical field strength**

The nucleus area of neural cells increased after electrical stimulation and is illustrated in Figure 4. It is clear from Figure 4 that the area of the nucleus and number of cells increased with increase in applied electrical field strength, with a maximum increase at 20 mV/mm stimulation, as compared to the control cells (no stimulation). However, a marked decrease was observed when the cells were stimulated at an applied electrical field strength of 50 mV/mm. There was a significant decrease in the number of proliferating cells cultured on CNT-PEDOT coated

stainless steel electrode. The effect of applied electrical field certainly affects the biophysicochemical functions of the stimulated cells such that the cellular proliferation and nuclear area is increased. Neuronal cells and excitable cells respond to changes in external field through voltage gated-ion channels. Their opening modifies the permeability of neuronal cells membrane and potentially leads to action potential. In contrast, electrical stimulation of non-excitabile cells promote alteration in extracellular ion concentration (including  $H^+$  and hence pH). This ultimately leads to alteration in electrochemical gradient across the plasma-membrane and promotes modification of membrane permeability to ions. Calcium signaling across the cells via connexins (other ion channels) is another possibility [23]. This affects the cell proliferation and metabolic activities, with higher rate of protein and DNA synthesis under the influence of applied electrical stimulation. Similarly, the applied electrical field had significant influence in the synthesis of actin, implying greater cytoplasmic extension and reorganization (see also section 4.3). The decrease in the number of cells at high electrical field strength is envisaged to be related to high current flow through the cells, which presumably alters the pH of the culture medium.

As shown in Figure 4b, the cell proliferation was significantly influenced by electrical stimulation. The cell proliferation increased with increase in the externally applied voltage. Highest neural cell proliferation was observed at 20 mV/mm. At electrical field greater than 20 mV/mm the cell death was observed

The higher proliferation of neural cells in the presence of an externally applied electrical field suggest non-toxic nature of the electrode material and positive effect of stimulation and the cells did not experience any observable cell death/apoptosis, as confirmed by MTT assay (Figure

5). It may be seen that after electrical stimulation, the cells remained viable and proliferated upto 72 hours (experimental study time).

The success of a neural prosthetic device is governed by the successful electrical stimulation of neural cells and the ability of the cells to attach to the surface of the CNT-PEDOT-coated stainless steel electrode. Figure 6 shows scanning electron microscopy micrographs of attached neural cells on the surface of CNT-PEDOT-coated electrode after electrical stimulation. The attachment of neural cells (control) can be seen in Figure 6a. In contrast, a number of cells were observed on electrical stimulation such that long neuritis extended and developed into extensive secondary processes. The extensive proliferation and branching in different directions and strong attachment to the surface with long neurite extension is indicative of an interface that is favorable for electrical stimulation. It also confirms the biocompatible nature of the surface that is favorable for growth of neural cells.

The average neurite length for neural cells cultured on PEDOT-CNT-coated electrode and subjected to electrical stimulation for 20 mV/mm was nearly quadrupled with control cells (no stimulation). This represents a 4 times increase in neurite length, which is significantly greater than the 2-3 times increase in neurite length observed for neural cells after stimulation at 5mV/mm and 10 mV/mm. Electrophoretic redistribution of cytoskeletal proteins or conformational changes in extracellular matrix proteins are responsible for the changes in the neurite length. In the present work, it is also shown that the electrical stimulation increases the expression level of proteins, actin and fibronectin. Among these, fibronectin is an extracellular matrix (ECM) adhesive glycoprotein and is crucial for the cellular attachment to the substrate surface. Hence, an enhanced ECM protein expression on electrical stimulation increases neuronal attachment and neurite outgrowth, as shown in Figure 6b.

In the SEM micrographs (Figure 6), the neurites were identified as elongated projections from the main cell body of neural cells. These elongated long fibers were in the range of 10-25  $\mu\text{m}$ , where the neurite length is governed by the electric field strength. At low field (5mV/mm), the average neurite length was  $\sim 10 \mu\text{m}$ , while at highest electrical field (20 mV/mm), the neurite length was increased from  $\sim 10 \mu\text{m}$  to 20  $\mu\text{m}$ , as shown in Figure 6b. Furthermore, the presence of neurites, which are indicator of viability and adhesion capability, of neural cells, confirmed that PEDOT-CNT is an excellent material for neural cells and can be used in neural tissue regeneration. The fiber-like thin projections are characteristic of neurites and neuronal outgrowth.

Neurite outgrowth is known to be induced by depolarization and a potential difference exists between the intracellular fluid of nerve cells [47]. When neural cells are inactive, the potential difference is nearly constant (steady), but on electrical stimulation, the cell membrane experiences an intensity-dependent depolarization. Once a threshold is attained, an action potential is generated that propagates across the membrane. Our results at 20 mV/mm indicate significant impact on neurite extension.

### **3.3 The impact of electric field stimulation on cytoskeleton proteins**

In this study, we have investigated the effects of the electrical field-induced cell-to-cell coupling behavior on protein synthesis and mechanisms by immunocytochemistry, keeping in mind that neuroblastoma cell line (NB-39-Nu), which has abundant adhesion proteins distributed through the cytoplasm. Different molecules play a significant role in cell motility and cell-to-cell contact [44,48, 49]. Actin is a primary cytoskeleton protein related to cellular mobility. Vinculin focal adhesion contact and actin contribute to morphological adhesive changes in cell [44, 48].

Immunocytochemical analysis of actin and vinculin is presented in Figure 7a. It may be noted from Figure 7a that the number of cells increased with electrical field strength from 5 mV/mm to 20 mV/mm, but at high electrical field strength of 50 mV/mm majority of the cells died, even though their nuclear area was greater than the control experiments (no stimulation). The expression level of primary cytoskeletal protein, actin, was increased with stimulation up to the electrical field strength of 20 mV/mm (Figure 7b), while that of vinculin was slightly decreased. The increase in actin expression suggests that the cell mobility was promoted or enhanced by the applied electrical field. On the other hand, the small decrease in vinculin expression implies that the focal adhesions formed at the interface between the cells and the CNT-PEDOT film were weakened and undermined because of the protrusion edge of contacting cell with the adjacent neighboring cells.

It is clear that the electric field influences the expression level of intracellular proteins, actin and vinculin, which contribute to cell mobility and cell adhesion, respectively and thereby enhances cell-to-cell contact beyond normal cell membrane protrusion. The aforementioned observations are of particular significance to neural cell transplantation therapy, given that cell therapy is being utilized to cure neuronal cell loss or neuronal functional loss [42].

Immunocytochemical analysis of extracellular matrix protein, fibronectin, in control neural cells (no simulation) and under electric field strength of 5 mV/mm is presented in Figure 8. An increase in the expression level of fibronectin suggests upregulation of fibrillar adhesions in the presence of electric field. The dissemination or distribution of fibronectin protein was changed from the wider sites in the cytoplasm to perinuclear location. This led to high concentration of fibronectin around the perinucleus (Figure 8). The localization of fibronectin in the center indicates that the cellular edge was actively modified to a greater degree in the

presence of electric field in contrast to the central cellular part. Cell-to-cell coupling is relevant in functional neuronal circuits and therefore, contributes the success of the transplantation [42].

The study described here provides a strong evidence and potential for consideration of CNT PEDOT-coated metallic microelectrodes (stainless or platinum) for neural stimulation. Besides the evidence of effect of electrical field on cytoskeleton proteins and cell-to-cell contact using CNT PEDOT-coated metallic steel electrodes, the microelectrode exhibited the desired attributes of stability, high charge injection limit, and low impedance at high frequency. The chemical and structural design of the microelectrode can be potentially extended to other microfabrication process related to neural electrodes such as microelectrochemical systems.

### **3.4 Implications of CNTs in neural tissue engineering**

Carbon nanotubes (CNTs) are being increasingly researched for neural tissue engineering applications and can be used in the design of neuronal interfaces or for synthesis of scaffolds to promote neuronal growth, as illustrated in our study. Given that the architecture of the scaffold structure is important in the success of implant, the introduction of longitudinal tubular structure such as that of CNTs provides physical guidance for axonal regrowth and cell migration and enhances nerve regeneration [50]. Based on the crucial role of process entanglements in neuronal anchoring, the appearance of a rough surface and large surface area of CNTs is expected to influence the contact between neuronal membrane and CNTs, and hence favorably impact direct electrical coupling [51].

The nanoscale roughness and its intrinsic conductivity render CNTs excellent candidate for neural tissue regeneration, because the nanotopography and physical and chemical properties of CNTs promote neural contact to CNTs, activating multiple and complex adhesion-mediated, intracellular signaling cascades [52]. In general, neural cells respond favorably to a surface

which consists of extracellular matrix components such as fibronectin, collagen, and laminin. In such a case, the neural cells first attach to the surface and with the help of biochemical cues, the dendrites start to elongate, while the extracellular signals stimulate the process of neurite outgrowth followed by the axonal growth. This means that the cell attachment and spreading is highly crucial for cell differentiation. In our case, the expression of ECM protein, fibronectin, provides favorable biochemical cues to stimulate neurite outgrowth.

Previous studies examined the relationship between CNTs and neuronal growth, and proposed that CNTs may affect neurite outgrowth [53]. However, we envisage that PEDOT may also induce signal transduction for neurite outgrowth. Thus, a detailed mechanism pertaining the role of CNTs and PEDOT in facilitating neural cell attachment and neurite outgrowth still needs to be determined. Similarly, the interaction of these components with intra and extracellular proteins requires further examination. These aspects are being currently studied and will be reported in future.

#### **4. Conclusions**

The study illustrates the potential and desired attributes of CNT-PEDOT-coated stainless steel electrodes for electrical stimulation of neural cells. The CNT-PEDOT-stainless steel electrodes were characterized by significantly low impedance ( $\sim 200$  ohm, at a frequency of  $10^5$  Hz compared to the bare electrode), high charge storage capacity, and a high charge injection limit of  $\sim 70$  mC/cm<sup>2</sup>. The CNT-PEDOT coated microelectrodes indicated no signs of delamination or cracking indicative of superior mechanical stability. The study of the effects of electrical field strength-induced stimulation of neural cells on protein synthesis and mechanism indicated cell-to-cell interaction. This implied change in the regulation of endogenous

cytoskeletal proteins, actin, vinculin, and fibronectin involving cell mobility and cell adhesion. The observed magnificent characteristics are promising for clinical trials.

### References

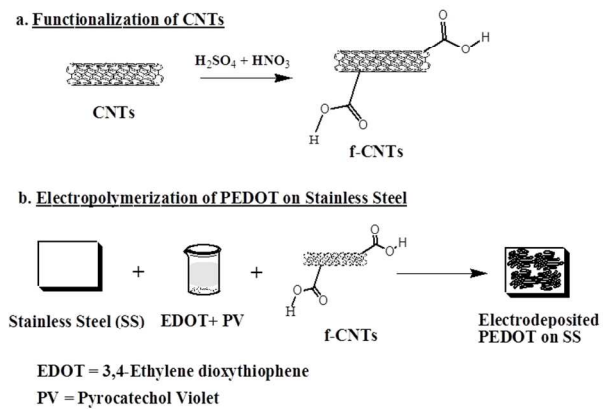
1. Wilson BS, Lawson DT, Muller JM, Tyler RS, Kiefer J. Cochlear implants: some likely next steps. *Ann. Rev Biomed. Eng.* 2003; 5: 207-49.
2. Weiland JD, Liu W, Humayun MS. Retinal prosthesis. *Ann. Rev. Biomed. Eng.* 2005; 7: 361-401.
3. Navarro X, Krueger TB, Lago N, Micera S, Stieglitz T, Dario P. A critical review of interfaces with the peripheral nervous system for the control of neuroprostheses and hybrid bionic systems. *J. Peripheral Nerv. Sys.* 2007; 10: 229.-58
4. Benabid AL. Deep brain stimulation for Parkinson's disease. *Curr. Opi. Neurobiol.* 2003; 13: 696-706.
5. Green RA, Suaning GJ, Poole-Warren LA, Lovell NL. Bioactive conducting polymers for neural interfaces: application to vision prosthetics. *International IEEE/ EMBS Conference Neural Engineering 2009*; 60-3.
6. Brummer SB, Turner MJ. Electrochemical considerations for safe electrical stimulation of the nervous system with Platinum electrodes. *IEEE Trans. Biomed. Eng.* 1997; 24: 59-63.
7. Winter JO, Cogan SF, Rizzo JF. 3rd. Retinal prostheses: current challenges and future outlook. *J. Biomaterials Sci. Polym. Ed.* 2007; 18: 1031-55.
8. Nam Y. Materials consideration for in vitro interface technology. *Mater. Res. Bull.* 2012; 37: 566-72.
9. Chen S, Allen MG. Extracellular matrix-based materials for neural interfacing. *Mater. Res. Bull.* 2012; 37: 606-19.
10. Di L, Wang LP, Lu YN, He L, Lin ZX, Wu KJ. Protein adsorption and peroxidation of rat retinas under stimulation of a neural probe coated with polyaniline. *Acta Biomaterialia* 2011; 7: 3738-45.

11. Lu Y, Cai ZX, Cao YL, Yang HX, Duan YY. Activated iridium oxide films fabricated by asymmetric pulses for electrical neural micro stimulation and recording. *Electrochem. Commun.* 2008; 10: 778-82.
12. Cogan SF, Guzelian AA, Agnew WF, Yuen TGH, McCreery DB. Over-pulsing degrades activated iridium oxide films used for intracortical neural stimulation. *J. Neurosci. Meth.* 2004; 137: 141-50.
13. Polikov VS, Tresco PA, Reichert WM. Response of brain tissue to chronically implanted neural electrodes. *J. Neurosci Methods.* 2005; 148: 1-18.
14. Zhong Y, Bellamkonda RV. Controlled release of anti-inflammatory agent  $\alpha$ -MSH from neural implants. *J. Control. Rel.* 2006; 106: 309-18.
15. Ordonez J, Schuetter M, Boehler C, Boretium T, Stieglitz T. Thin films as microelectrode array for neuroprosthetics. *Mater. Res. Bull.* 2012; 37: 590-8.
16. Merrill DR, Bikson M, Jefferys JGR. Electrical stimulation of excitable tissue: design of efficacious and safe protocols. *J. Neurosci. Methods* 2005; 141: 171-98.
17. Rose TL, Robblee LS. Electrical-stimulation with Pt electrodes. VIII. Electrochemically safe charge injection limits with 0.2 ms pulses. *IEEE Trans. Biomed. Eng.* 1990; 37: 1118-20.
18. Keefer EW, Botterman BR, Romero MI, Rossi AF, Gross GW. Carbon nanotube coatings improves neuronal recordings. *Nat. Nanotechnol.* 2008; 3: 434-9.
19. Weiland JD, Anderson DJ. Chronic neural stimulation with thin-film, iridium oxide electrodes. *IEEE Transactions Biomed. Eng.* 2000; 47: 911-8.
20. Gobbels K, Kuenzel T, Ooyen AV, Baumgartner W, Schnakenberg U, Braunig P. Neuronal cell growth on Iridium Oxide. *Biomaterials* 2010; 31: 1055-67.
21. Lee I, Whang CN, Choi K, Choo MS, Lee YH. Characterization of iridium film as a stimulating neural electrode. *Biomaterials* 2002; 23: 2375-80.
22. Mailley SC, Hyland M, Mailley P, McLaughlin JM, E.T. McAdams. Electrochemical and structural characterizations of electrodeposited iridium oxide thin-film electrodes applied to neuro stimulating electrical signal. *Mater. Sci. Eng. C: Biomater. Sci.* 2002; 21: 167-75.

23. Zeng Y, Lu XH, Zeng SQ, Tian SL, Li M, Shi J. Sustained depolarization-induced propagation of  $[Ca^{2+}]$  oscillations in cultured DRG neurons: The involvement of extracellular ATP and P2Y receptor activation. *Brain Res.* 2008; 1239: 12-23.
24. Hung LY, E. Neher.  $Ca^{2+}$  dependent exocytosis in the somata of dorsal root ganglion neurons. *Neuron* 1996; 17: 135-45.
25. Zhang C, Xiong W, Zheng H. Calcium-and dynamin-independent endocytosis in dorsal root ganglion neurons. *Neuron* 2004; 42: 225-36.
26. Ouyang K, Zheng H, Qin X, Zhang C, Yang D, Wang X, Wu C, Zhou Z, Cheng H.  $Ca^{2+}$  sparks and secretion in dorsal root ganglion neurons. *Proc. Natl. Acad. Sci. USA* 2005; 23: 12259-64.
27. Baek S, Green R, Granville A, Martens P, Poole-Warren L. Thin film hydrophilic electroactive polymer coatings for bioelectrodes. *J. Mater. Chem. B* 2013; 1: 3803-10.
28. Jan E, Hendricks JL, Husaini V, Richardson-Burns SM, Sereno A, Martin DC, Kotov NA. Layered Carbon Nanotube-Polyelectrolyte Electrodes Outperform Traditional Neural Interface Materials. *Nano Lett.* 2009; 9: 4012-8.
29. Benfenati V, Toffanin S, Bonetti S, Turatti G, Pistone A, Chiappalone M, Sagnella A, Stefani A, Generali G, Ruani G, Saguatti D, Zamboni R, Muccini M. A transparent organic transistor structure for bidirectional stimulation and recording of primary neurons. *Nat. Mater.* 2013; 12: 672-80.
30. Cramer T, Chelli B, Murgia M, Barbalinardo M, Bystrenova E, de Leeuw DM, Biscarini F. Organic ultra-thin film transistors with a liquid gate for extracellular stimulation and recording of electric activity of stem cell-derived neuronal networks. *Phys. Chem. Chem. Phys.* 2013; 21: 3897-905.
31. Seifert G, Schilling K, Steinhauser C. Astrocyte dysfunction in neurological disorders: a molecular perspective. *Mat. Rev. Neurosci.* 2006; 7: 194-206.
32. Nagelhus EA, Amiry-Moghaddam M, Bergersen LH, Bjaalie JG, Eriksson J, Gundersen V, Leergaard TB, Morth JP, Storm-Mathisen J, Torp R, Walhovd KB, Tonjum T. The glia doctrine: addressing the role of glial cells in healthy brain ageing. *Mach Ageing Dev.* 2013; 134: 449-599.
33. Benfenati V, Martino N, Antognazza MR, Pistone A, Toffanin S, Ferroni S, Lanzani G, Muccini M. Photostimulation of whole-cell conductance in primary rat neocortical

- astrocytes mediated by organic semiconducting thin films. *Adv. Healthc. Mater.* (DOI No. 10.1002/adhm.201300179).
34. Groenendaal BL, Jonas F, Freitag D, Pielartzik H, Reynolds JR. Poly(3,4-ethylenedioxythiophene) and its derivatives: past, present, and future. *Adva. Mater.* 2000; 12: 481-94.
  35. Chao TI, Xiang S, Chen CS, Chin WC, Nelson AJ, Wang C. Carbon nanotubes promote neuron differentiation from human embryonic stem cells. *Biochem. Biophys. Res. Commun.* 2009; 384: 426-30.
  36. Matsumoto K, Sato C, Naka Y, Whitby R, Shimizu N. Stimulation of neuronal neurite outgrowth using functionalized carbon nanotubes. *Nanotechnol.* 2010; 21: 115101.
  37. Cellot G, Cilia E, Cipollone S, Rancic V, Sucapane A, Giordani S. Carbon nanotubes might improve neuronal performance by favoring electrical shortcuts. *Nature Nanotechnol.* 2009; 4: 126-33.
  38. Hu H, Ni Y, Mandal SK, Montana V, Zhao B, Haddon R.C. Polyethyleneimine functionalized single-walled carbon nanotubes as a substrate for neuronal growth. *J. Phy. Chem. B* 2005; 109: 4285-9.
  39. Luo X, Weaver CL, Zhou DD, Greenberg R, Cui XT. Highly stable carbon nanotube doped Poly(3,4-ethylenedioxythiophene) for chronic neural stimulation. *Biomaterials* 2011; 32: 5551-7.
  40. Wang K, Fishman HA, Dai H, Harris JS. Neural stimulation with a carbon nanotube microelectrode assay. *Nano Lett.* 2006; 6: 2043-8.
  41. Lu Y, Li T, Zhao X, Li M, Cao Y, Yang H. Electrodeposited electrodes for neural interfaces. *Biomaterials* 2010; 31: 5169-81.
  42. Heo C, Yoo J, Lee S, Jo A, Jung S, Yao H, Lee YH, Suh M. The control of neural cell-to-cell interactions through non-contact electrical field stimulation using graphene electrodes. *Biomaterials* 2011; 32: 19-27.
  43. Jan E, Hendricks JL, Husaini V, Richardson-Burns SM, Serene A, Marten DC. Layered carbon nanotubes polyelectrolyte electrodes outperform traditional neural interface materials. *Nano Lett.* 2009; 9: 4012-8.
  44. Cui XT, Zhou DD. Poly (3,4-ethylenedioxythiophene) for chronic neural stimulation. *IEEE Trans Neural Rehabil. Eng.* 2007; 15: 502-8.

45. Bobacka J, Lewenstam A, Ivaska A. Electrochemical impedance spectroscopy of oxidized poly (3,4-ethylene dioxythiophene) film electrodes in aqueous solution. *J. Electroanal. Chem.* 2000; 489: 17-27.
46. Macdonald JR. Impedance spectroscopy: emphasizing solid materials and systems. New York; Wiley: 1987.
47. Matthews G. Cellular Physiology of nerve and muscle, 4th Edition. Blackwell Science Ltd., Malden, MA, 2003.
48. Small JV, Geiger B, Kaverina I, Bershadsky A. How do microtubules guide migrating cells? *Nat. Rev. Mol. Cell Biol.* 2002; 3: 957-64.
49. Morgan MR, Humphries MJ, Bass MD. Synergistic control of cell adhesion by integrins and syndecan. *Nat. Rev. Mol. Cell Biol.* 2007; 8: 957-69.
50. Spivey FC, Khaniz, ZZ, Shear JB, Schmidt CE. The fundamental role of subcellular topography in peripheral nerve repair therapies. *Biomaterials* 2012; 33: 4264-4276.
51. Cellot G, Cilia E, Cipollone S, Rancic V, Sucapane A. et al. Carbon nanotubes might improve neuronal performance by favoring electrical shortcuts. *Nat. Nanotechnol.*, 2009; 4: 126-133.
52. Dvir T, Timko BP, Kohane DS, Langer R. Nanotechnological strategies for engineering complex tissues. *Nat. Nanotechnol*, 2011; 6: 13-22.
53. H. Hu, Y. Ni, V. Montana, R.C.Haddon, V. Parpura. Chemically functionalized carbon nanotubes as substrates for neuronal growth. *Nano Lett.* 2004; 4 (3): 507-11.



Scheme 1. Schematic illustration of fabrication of neural electrode. (a) Functionalization of carbon nanotubes (CNTs) by acid based oxidation to generate functionalized CNTs (f-CNTs). (b) Electropolymerization of 3,4-dioxythiophene (EDOT) on stainless steel (SS) in the presence of pyrocatechol violet (PV).  
338x190mm (96 x 96 DPI)

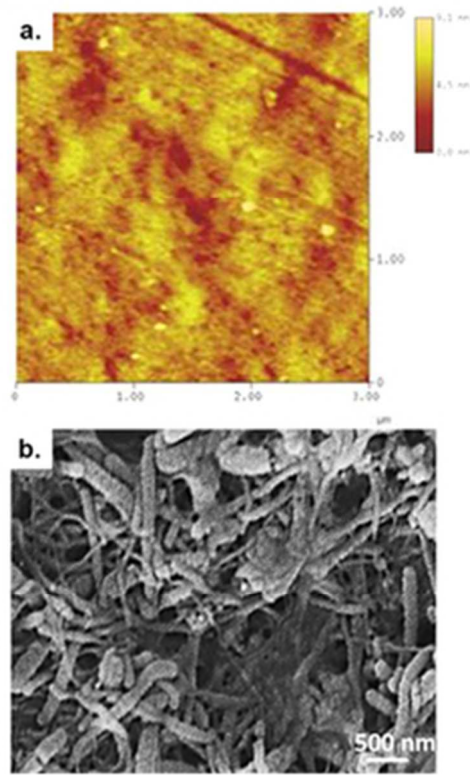


Figure 1. (a) Atomic force micrographs of austenitic stainless steel obtained in tapping modes using a scan area of  $3 \times 3 \mu\text{m}^2$ . The average roughness of coarse-grained steel is  $1.45 \pm 0.21 \text{ nm}$ . (b) Scanning electron micrograph of PEDOT/CNT coated stainless steel microelectrode. There was uniform distribution of CNTs coated with PEDOT in the polymer matrix  
20x33mm (300 x 300 DPI)

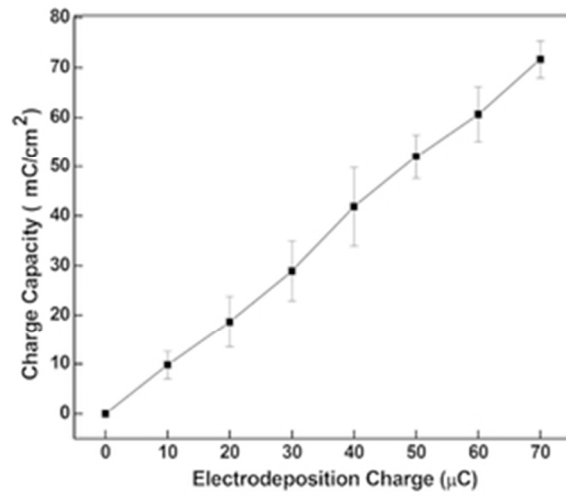


Figure 2. The charge capacity of CNT-PEDOT coated stainless steel electrode as a function of the CNT-PEDOT electrodeposition charge. Bars represented the range over which the values were measured.  
25x22mm (300 x 300 DPI)

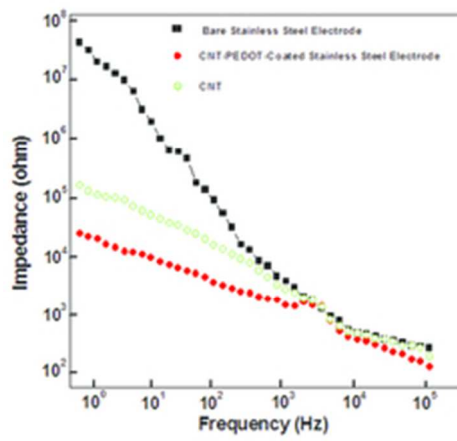


Figure 3. Electrochemical impedance of bare stainless steel, CNT-coated stainless steel, and CNT-PEDOT coated-stainless steel electrodes. 20x19mm (300 x 300 DPI)

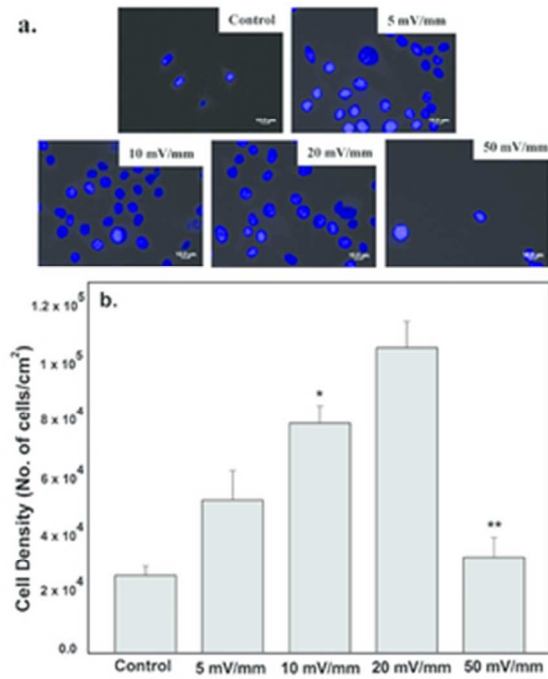


Figure 4. (a) 4',6-diamidino-2-phenylindole (DAPI) stained proliferation of neural cells on CNT-PEDOT coated stainless steel electrode as a function of electrical field strength. At high electrical field strength of 50 mV/mm, the high pH of the culture media is altered that leads to cell death/apoptosis, (b) Quantification of cell proliferation via estimation of cell density in fluorescence micrographs. Asterisk mark (\*) represents significant difference among the control and sample at  $p < 0.05$  and bars represent to standard deviation, while (\*\*) corresponds to significant difference among the stimulated samples 25x31mm (300 x 300 DPI)

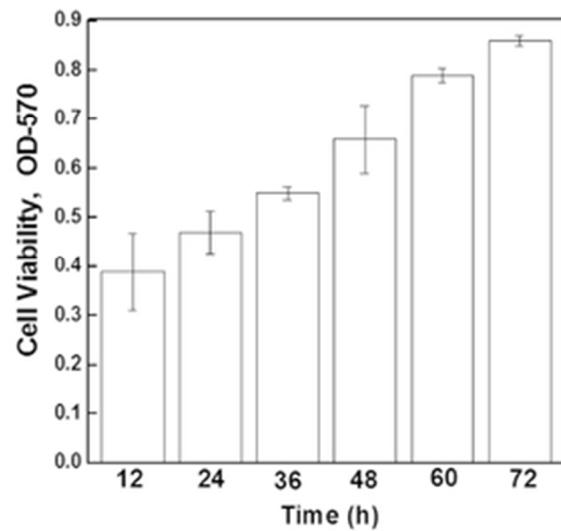


Figure 5. Non-cytotoxicity of the CNT-PEDOT coated stainless steel electrode and cell proliferation as determined through MTT assay. Excellent viability and proliferation of neural cells on CNT-PEDOT coated stainless steel electrode on electrical stimulation at a 10 mV/mm is noted. Bars represent the range over which the values were measured. Asterisk mark (\*) represents significant difference among the control and sample at  $p < 0.05$  and bars represent to standard deviation, while (\*\*) corresponds to significant difference among the stimulated samples.  
25x23mm (300 x 300 DPI)

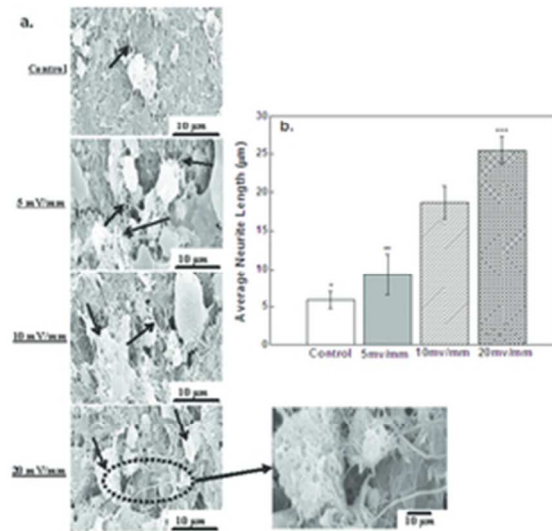


Figure 6. (a) Scanning electron micrographs of differentiated and proliferated neural cells on CNT-PEDOT coated stainless steel electrodes illustrating the effect of applied electrical field strength on neurites (arrows) and extensive branches (circle) that attach to the substrate surface. The scale bar in all micrographs is 10 µm. (b) average neurite lengths of neural cells cultured and electrically stimulated on PEDOT-CNT coatings and control cells (no stimulation). Bars in Figure (b) represent the range over which the values were measured. Asterisk mark (\*) represents significant difference among the control and sample at  $p < 0.05$  and bars represent to standard deviation, while (\*\*) corresponds to significant difference among the stimulated samples.

25x25mm (300 x 300 DPI)

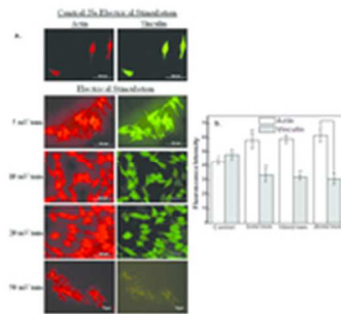


Figure 7. (a) Immunocytochemical analysis of actin and vinculin in neural cells (neuroblastoma cell line: NB-39-Nu) under no stimulation (control) and under different electrical field strength stimulation and (b) quantitative analysis of fluorescence intensity of control cells and electrically stimulated cells. Bars in (b) represent the range over which the values were measured. Asterisk mark (\*) represents significant difference among the control and sample at  $p < 0.05$  and bars represent to standard deviation, while (\*\*) corresponds to significant difference among the stimulated samples.  
15x13mm (300 x 300 DPI)

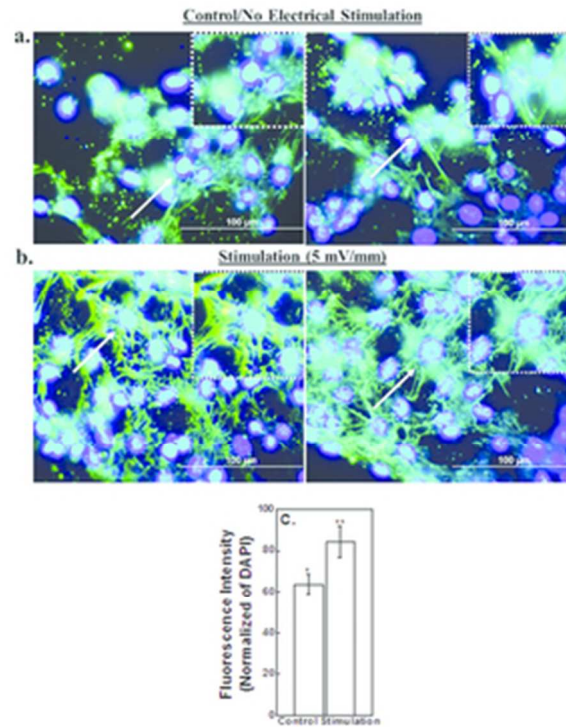
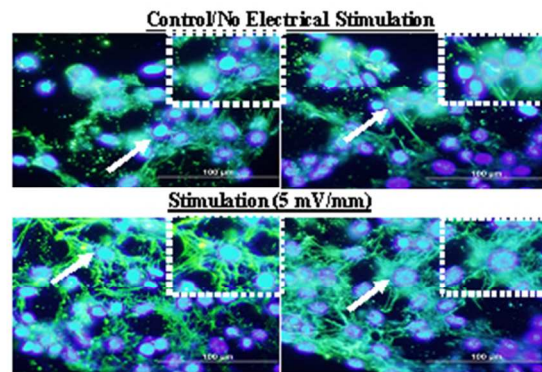


Figure 8. Immunocytochemical analysis of fibronectin in (a) neural cells (neuroblastoma cell line: NB-39-Nu) under no stimulation and (b) electrically stimulated cells (5 mV/mm). The inset is the magnified view of the region marked with the white arrow. (c) The histogram depicts quantitative expression level of fibronectin analyzed using Image Pro software. The values are mean  $\pm$  SD ( $n = 5$ ). Asterisk mark (\*) represents significant difference among the control and sample at  $p < 0.05$  and bars represent to standard deviation, while (\*\*) corresponds to significant difference among the stimulated samples.  
25x32mm (300 x 300 DPI)



Electrical stimulation induced cytoskeletal proteins reorganization of neural cells on PEDOT-CNT coated stainless steel neural probe.  
211x211mm (72 x 72 DPI)